ChemComm

COMMUNICATION

View Article Online
View Journal | View Issue

One-step hydrothermal amino-grafting of graphene oxide as an efficient solid base catalyst†

Cite this: *Chem. Commun.*, 2014, **50**, 4305

Received 16th December 2013,
Accepted 2nd March 2014

DOI: 10.1039/c3cc49529a

www.rsc.org/chemcomm

Yicheng Zhang,[a] Chunlin Chen,[b] Guangjun Wu,[a] Naijia Guan,[a] Landong Li*[a] and Jian Zhang*[b]

A one-step hydrothermal route is developed to prepare amino-grafted graphene oxide as an environmentally benign heterogeneous solid base catalyst.

With the developments in metal-free carbon catalysis and graphene materials, the catalytic applications of graphene and its precursor graphite oxide have been widely investigated in a variety of reactions.[1] The most attractive property of a graphene-based material as the catalyst is its controllable surface properties allowing the functionalization of active groups. For instance, the sulfonated graphene was applied as a water-tolerant solid acid catalyst and showed a high activity in hydrolysis of ethyl acetate.[2] It is possible to graft nitrogen atoms on the matrix of graphene sheets and thus endue the carbon solid with the surface basicity. More examples of N-incorporated nanocarbons for base catalysis can be related to carbon nanotubes (CNTs).[3] Bitter and his co-workers used N-doped CNTs to catalyze the Knoevenagel condensation between benzaldehyde and ethylcyanoacetate, and found that the activity was determined by the amount of pyridinic N components.[3a] Tessonnier *et al.* applied amino-grafted CNTs as a solid base catalyst for transesterification of glyceryl tributyrate with methanol and observed a superior activity to the commercial hydrotalcite.[3b] A survey of the literature shows that the use of N-incorporated graphene as a base catalyst has been still limited in several specific reactions, *i.e.* hydrolysis of ethyl acetate,[1c] and, importantly, there is still a lack of fundamental research into the working mechanism of graphene base catalysis.

Amino-grafting of carbon materials is performed *via* the consecutive deprotonation–carbometalation by *n*-BuLi followed by an electrophilic substitution with bromotriethylamine or 2-diethylaminoethylbromide, which is usually conducted under the dry conditions.[1c] Another route is oxidation–amination but it suffers from the remaining acidic functional groups being prone to catalyze side-reactions.[3b] In addition, the use of a hazardous reagent like *n*-BuLi or $SOCl_2$ inevitably results in a high capital cost and complicated procedures. Herein we report a convenient and cheap route to graft the as-synthesised graphene oxide (GO) with large amounts of nitrogen-containing groups. In principle, the GO was produced from graphite according to the Hummers method with some modifications.[4] The GO was dispersed into the aqueous solution of primary amines and then transferred into an autoclave for hydrothermal treatment at 333–453 K. The amino-grafted GO materials were labeled as MAGO (methylamine), EAGO (ethylamine), PAGO (propylamine) and BAGO (butylamine).

The morphological properties of GO and the representative amino-functionalized GO (PAGO) were determined by means of AFM and TEM. The AFM image in Fig. 1a reveals that the lateral dimensions of the as-prepared GO ranged between several hundred

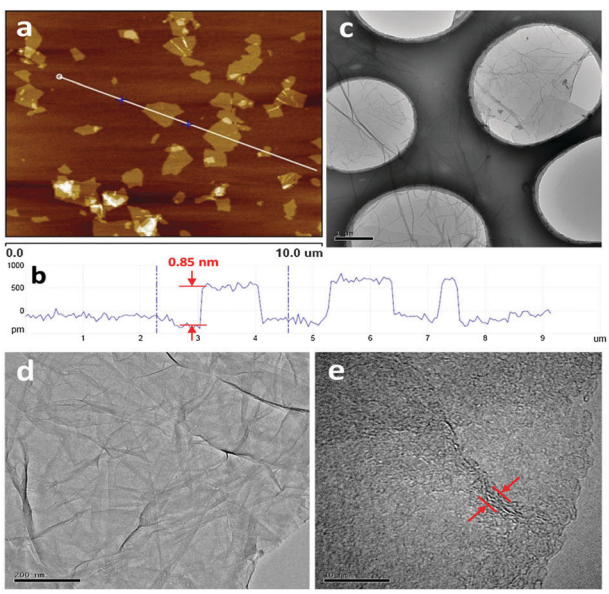

Fig. 1 AFM (a, b) and TEM (c) images of GO and TEM images of PAGO (d, e).

[a] *Key Laboratory of Advanced Energy Materials Chemistry (Ministry of Education), College of Chemistry, Nankai University, Tianjin 300071, P.R. China. E-mail: lild@nankai.edu.cn; Tel: +86-22-23500341*

[b] *Department of New Energy Technology, Ningbo Institute of Materials Technology & Engineering, Chinese Academy of Sciences, Ningbo 315201, P.R. China. E-mail: jzhang@nimte.ac.cn; Fax: +86-574-87615956*

† Electronic supplementary information (ESI) available: Experimental details and more characterization results. See DOI: 10.1039/c3cc49529a

nanometers and several micrometers. The apparent thickness was about 0.85 nm (Fig. 1b), corresponding to the monolayer GO sheet.[5] The thickness of GO is much larger than that of monolayer graphene (0.34 nm) due to the presence of oxygen functional groups at the periphery or in the basal plane of GO.[6] The TEM image in Fig. 1c shows a typical crumpling structure, indicating that the GO sheet is flexible. After propylamine functionalization, the morphology of GO was well preserved and a flexible PAGO sheet can be observed (Fig. 1d). The high resolution TEM image of PAGO in Fig. 1e reveals the existence of 3–4 layers in the PAGO nanosheet. The interlayer spacing was calculated to be *ca.* 0.5 nm, which is higher than that of monolayer graphene but lower than that of monolayer GO, indicating that graphene oxide was partially reduced by removing oxygen-containing functional groups during the reaction. The functionalized GO layers were crumpled, interrupted and full of defects, allowing the catalytic use with great accessibility to the reactant molecules.

We applied Raman and XPS techniques to characterize structural and surface properties of graphene materials. As seen in Fig. S1a (ESI†), GO and grafted GO show similar strong disorder-induced D bands, in-plane vibration of the graphene lattice G bands and their overtones (2D, D + G and 2G). It is accepted that the intensity ratio of the D and G bands (I_D/I_G) is inversely proportional to the density of defects of graphene-based materials.[7] After the hydrothermal treatment, the measured I_D/I_G ratio of GO increased from 1.01 to 1.17, 1.22, and 1.20 for MAGO, EAGO, and PAGO, respectively. Such a decrease in ordering of carbon atoms can be majorly related to the functionalization of amino groups *via* covalent bonds,[8] as confirmed by the XPS results in Fig. S1b (ESI†). The intensive peak centering at *ca.* 400.0 eV clearly proved the existence of grafted N atoms in the treated GO samples. Elemental analysis shows that the total contents of nitrogen are 18.0, 10.8 and 8.6% for MAGO, EAGO and PAGO, respectively. The reason for the difference in grafting efficiency could be attributed to the effect of chain length in primary amines that may affect the reactivity with oxygen groups in graphene sheets. The hydrothermal treatment also resulted in a significant decrease of the oxygen content from 24.1% to 7.9–9.3%, probably due to the partial reduction of GO.

The C1s and N1s spectra of GO and amino-grafted GO are illustrated in Fig. 2. Typically, the C1s profile of GO can be fitted by three elementary peaks, *i.e.* 284.8, 286.8 and 288.1 eV, corresponding to sp^2 C, C–O groups, and C═O groups, respectively (Fig. 2a). For amino-grafted GO, the intensities of C–O and C═O groups decreased distinctly while the signal of C–N groups appeared at 284.5 eV, clearly indicating that the functionalization of GO is mainly achieved *via* reaction with oxygen groups to form C–N bonds. The N1s spectra of amino-grafted GO samples (Fig. 2b) comprise three components, *i.e.* pyridinic N,[5,9a] amine N[9b,c] and ammonium N[9d] centering at 398.4, ~400.0 and 402.1 eV, respectively. Deconvolution identified the prevailing fraction of grafted amine N species, confirming the major pathway of C–N formation *via* the binding of amines at the C–O sites.

Thermal stability of surface functional groups is one of the most important properties of a catalyst. TG-MS profiles of GO and amino-functionalized GO are shown in Fig. 3. In agreement with the previous reports,[10] the major weight loss (~27%) of GO at around 473 K was assigned to the release of CO_x and H_2O from the labile oxygen groups. The weight loss between 500 and 950 K might be related to the removal of more stable oxygen functional groups.[11] The desorption profiles of functional groups changed a lot after the treatment with primary amines. First, the weight loss of amino-grafted GO below 500 K was less than 6% and the amount of CO_x greatly reduced, revealing the reduced number of oxygen species. Second, the stability of functional groups was improved and the peak maximum in DTG curve shifted upwards (Fig. 3b). Desorption profiles of CO and CO_2 became more dispersive and the less stable components centering at around 520 K almost disappeared (Fig. 3c). As shown in Fig. 3d, the length of the carbon chain in the primary amines can significantly affect the stability of amino groups, *i.e.* the shorter the carbon chain the higher the desorption temperature. Typically, the release of methylamine, ethylamine and propylamine from MAGO, EAGO and PAGO started at *ca.* 800 K, 600 K and 500 K, respectively. The amine groups in functionalized GO are thermally

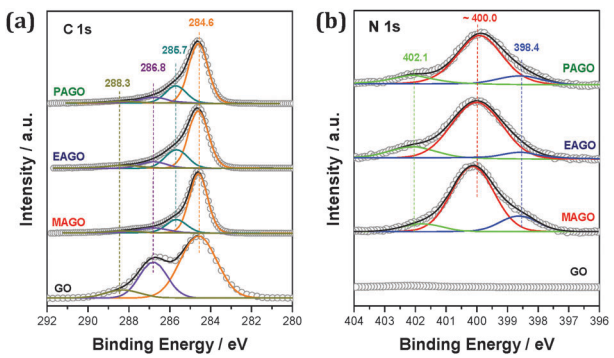

Fig. 2 High-resolution C1s (a) and N1s (b) XP spectra of GO and amine-functionalized GO.

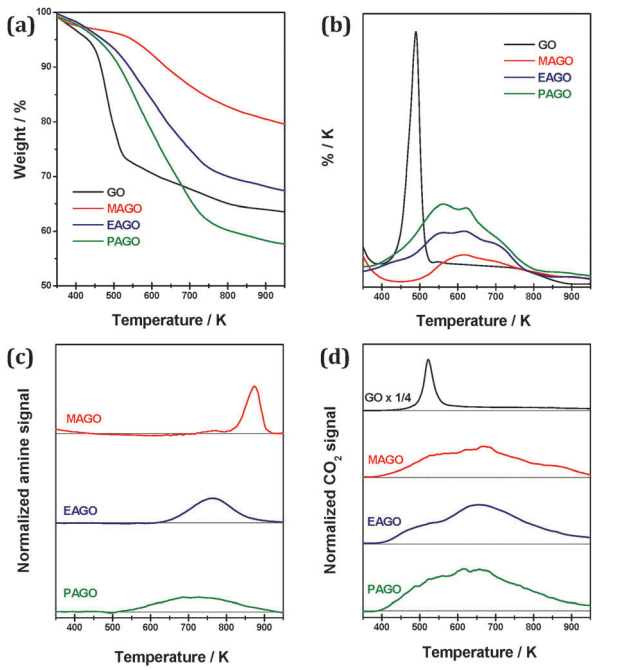

Fig. 3 TG-MS results of GO and amine-grafted GO: TG (a) and DTG (b) profiles, the MS signal of released CO_2 (c) and amines (d).

stable at below 500 K, allowing their applications in a variety of catalytic reactions. It is even possible to use MAGO as the catalyst or inert support for some gas-phase reactions at temperatures lower than 800 K.

Due to the environmentally friendly and sustainable properties, functionalized carbon materials have been applied as the solid acid or base catalysts. For example, amine modified carbon nanotubes exhibited a high catalytic activity in transesterification reaction.[3b] In this work, the basicity of amino-functionalized GO was roughly analyzed by using different Hammett indicators. The results showed that all amino-grafted GO materials are super bases by processing basic sites with pK_a values of 37–39. Amino-grafted GO is first tested as a catalyst for the Knoevenagel condensation reaction. The reaction between benzaldehyde and methylene cyanide is very quick and ~100% benzaldehyde conversion can be obtained within 4 hours using all amino-grafted GO as the catalyst. If diethyl malonate was used as a reactant instead of methylene cyanide, the reaction rate was lowered and benzaldehyde conversion of 22.1, 28.3 and 53.2% was obtained catalyzed by MAGO, EAGO and PAGO, respectively. The reason was attributed to the higher stereo-hindrance of diethyl malonate than that of methylene cyanide when reacting with benzaldehyde. No by-products or derivatives from amino-grafted GO can be identified by GC-MS analysis, indicating that the reaction was indeed a heterogeneous catalysis process and the GO samples were effective catalysts for the Knoevenagel condensation reaction. On the basis of reaction data, we proposed that the order of overall basic strength should be PAGO > EAGO > MAGO.

The activity of functionalized GO was further tested in Michael addition and transesterification reaction. In Michael addition reaction, nitromethane reacts with methylacrylate to yield methyl 4-nitrobutanoate as the main product. The methylacrylate conversion was as low as 6% without any catalyst but dramatically increased to 53.1% when MAGO was used as the catalyst. The conversion was 37.9 and 24.2% for EAGO and PAGO, respectively. KF/Al_2O_3 is a kind of super strong solid base catalyst and its Hammett value is nearly the same as amino-functionalized GO.[12] When we used KF/Al_2O_3 (2 mmol g^{-1}, equal to the N content in amino-functionalized GO) as the catalyst, the methylacrylate conversion is 47.0% ranking behind MAGO but before EAGO or PAGO. From the research on Michael addition reaction, we know that an amine is apt to react with nitromethane even at room temperature and thus all amine-type N species are totally blocked by nitromethane during the reaction. Therefore, the catalytic activity of amino-grafted GO should mainly originate from pyridinic N species, especially taking into account the relatively low basicity of ammonium N species.

In transesterification, methyl benzoate reacts with excess ethylene glycol to produce ethylene glycol acetate benzoate. It is seen that methyl benzoate conversion increased with the reaction time for all amine-functionalized GO samples (Fig. S2, ESI†). After 42 h, the reaction nearly completed and all grafted GO catalysts displayed the selectivity of *ca.* 96%. The analysis of the reactant by GC-MS showed the absence of leached amines or other derivatives, confirming a good stability of active components under the reaction conditions. The methyl benzoate conversion at 8 h was chosen to compare the activity of different samples. The conversion was as low as 2% without the presence of any catalyst. When amino-grafted GO was used as a catalyst, the methyl benzoate conversion ranged between 45 and 70% and PAGO exhibited the highest catalytic activity. It is known that the alkyl group can donate electrons to the N atom in amine and the electrophobic effect will strengthen the basicity. Generally, long carbon chains will make the electron donation easy and thus enhance the basicity. BAGO should possess the strongest basicity and exhibit the highest activity. However, with the increasing length of the carbon chain, the steric effect becomes intensive and the transesterification reaction will be obstructed. PAGO showed the highest basic catalytic activity as a result of balancing these two important factors. We note that PAGO even exhibited a higher activity than pure *n*-propylamine (54% methyl benzoate conversion at 8 h), which can be explained by the possibility that the linkage on the graphene matrix as a big π-conjugated system may benefit the transformation of primary amine into tertiary amine to result in an enhanced basicity.

To elucidate the working mechanism of surface functional groups, we attempted to correlate the catalytic activity with the quantitative analysis of N species by the high-resolution XPS. A series of PAGO samples were prepared hydrothermally at different synthesis temperatures (denoted as PAGO-*t*) and evaluated in Michael addition and transesterification reactions. For the PAGO-333 sample, the deconvolution of the N1s spectrum shows two major components at 399.9 and 402.1 eV, being assigned to amine and ammonium N, respectively, (Fig. S3, ESI†). Upon increasing the hydrothermal temperature, the elementary peak at 398.4 eV corresponding to pyridinic N species became intense. As seen in Table 1, the fraction of pyridinic N increases from 0.39 to 1.54% with the increase in synthesis temperature from 333 to 453 K. The amount of amine N species distributed rather randomly and the maximum of 6.12% appeared at hydrothermal temperature of 353 K. In contrast, the oxygen functional groups started to decompose at 373 K, which is detrimental to the reaction between the epoxy group and amine. The molecular water may compete with amine in reacting with the epoxy group at high temperature, leading to the decrease in the percentage of total N and amine N species.

For the Michael addition reaction, PAGO-333 seems to be inactive after background subtraction, *i.e.* 6% in the blank experiment. The methylacrylate conversion gradually increased

Table 1 The contents of specific N species in PAGO and the catalytic activities in the Michael addition and transesterification reaction

	Surface N content[a]/%			Conversion/%	
Sample	Total	Pyridinic	Amine	Michael addition	Transesterification
Blank	—	—	—	6	2
PAGO-333	6.3	0.39	5.16	6	65
PAGO-353	8.6	0.99	6.12	25	70
PAGO-373	8.5	1.06	4.47	29	58
PAGO-393	7.3	1.08	3.78	30	50
PAGO-423	6.6	1.45	4.04	43	55
PAGO-453	6.3	1.54	3.92	49	53

[a] N content was determined by XPS.

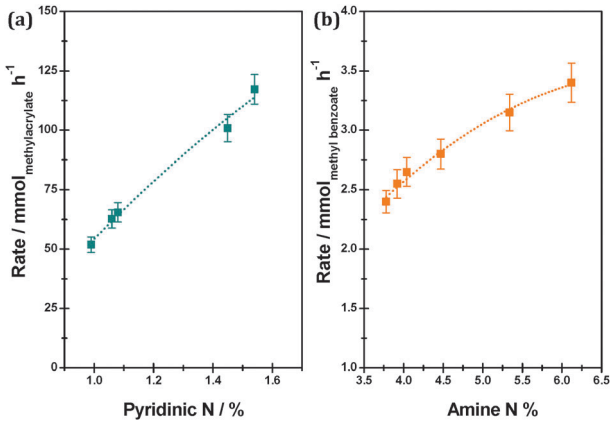

Fig. 4 Correlation between the specific N content in PAGO and the catalytic activity.

from 6 to 49% with the increase in synthesis temperature, being similar to the change in the amount of pyridinic N. A direct correlation between the fraction of pyridinic N and the methylacrylate conversion was obtained (Fig. 4a), indicating a determining role of the pyridinic N component especially after ruling out the effect of amine N as discussed above. For transesterification reaction, both pyridinic N and amine N showed certain basicity, and their contributions to the activity are difficult to be distinguished. To solve the problem, we passivated the amine species in PAGO-*t* samples with nitromethane at the reaction temperature (323 K for 12 h, followed by drying overnight under vacuum at 323 K) before transesterification. The nitromethane treated PAGO-*t* catalysts surprisingly displayed no activity in transesterification reaction, while the activity in Michael addition reaction was well preserved. We therefore concluded that the amine N should be the actual active component for transesterification reaction, as confirmed by the proportional relationship between the content of amine N and the conversion rate of methyl benzoate (Fig. 4b).

To sum up, we demonstrate a facile and economical route to functionalize GO by nitrogen-containing groups *via* hydrothermal treatment in the aqueous solution of primary amines. The amount of total nitrogen atoms and the distribution of nitrogen components can be well adjusted by controlling the synthesis parameters like the type of amines and hydrothermal temperature. The amino-grafted GO samples displayed a super basicity with the apparent pK_a value of 37–39 and exhibited remarkable catalytic activities in several typical homogeneous reactions, *i.e.* Knoevenagel condensation, Michael addition and transesterification. The amine N species coordinated the transesterification reaction between methyl benzoate and ethylene glycol, while pyridinic N species were responsible for the Michael addition between nitromethane and methylacrylate. The as-obtained amino-grafted GO is proved to be a kind of environmentally benign heterogeneous solid base catalyst that can be applied to a series of base-catalysed reactions.

This work was supported by the Collaborative Innovation Center of Chemical Science and Engineering (Tianjin), the Ministry of Education of China (NCET-11-0251 and IRT13022), 111 Project (B12015) and the National Natural Science Foundation of China (51202262, 50921004, and 21133010).

Notes and references

1 (*a*) J. Liang, Y. Jiao, M. Jaroniec and S. Z. Qiao, *Angew. Chem., Int. Ed.*, 2012, **51**, 11496; (*b*) S. Yang, X. Feng, X. Wang and K. Müllen, *Angew. Chem., Int. Ed.*, 2011, **50**, 5339; (*c*) C. Yuan, W. Chen and L. Yan, *J. Mater. Chem.*, 2012, **22**, 7456; (*d*) S. Verma, H. P. Mungse, N. Kumar, S. Choudhary, S. L. Jain, B. Sain and O. P. Khatri, *Chem. Commun.*, 2011, **47**, 12673; (*e*) D. R. Dreyer, R. S. Ruoff and C. W. Bielawski, *Angew. Chem., Int. Ed.*, 2010, **49**, 9336; (*f*) D. R. Dreyer and C. W. Bielawski, *Chem. Sci.*, 2011, **2**, 1233; (*g*) D. R. Dreyer and C. W. Bielawski, *Adv. Funct. Mater.*, 2012, **22**, 3247; (*h*) D. W. Boukhvalov, D. R. Dreyer, C. W. Bielawski and Y. W. Son, *ChemCatChem*, 2012, **4**, 1844; (*i*) H. P. Jia, D. R. Dreyer and C. W. Bielawski, *Adv. Synth. Catal.*, 2011, **353**, 528; (*j*) D. R. Dreyer, K. A. Jarvis, J. F. Paulo and C. W. Bielawski, *Macromolecules*, 2011, **44**, 7659; (*k*) D. R. Dreyer, K. A. Jarvis, P. J. Ferreira and C. W. Bielawski, *Polym. Chem.*, 2012, **3**, 757; (*l*) A. D. Todd and C. W. Bielawski, *Catal. Sci. Technol.*, 2013, **3**, 135.
2 J. Ji, G. Zhang, H. Chen, S. Wang, G. Zhang, F. Zhang and X. Fan, *Chem. Sci.*, 2011, **2**, 484.
3 (*a*) S. van Dommele, K. P. de Jong and J. H. Bitter, *Chem. Commun.*, 2006, 4859; (*b*) J. P. Tessonnier, A. Villa, O. Majoulet, D. S. Suand and R. Schlögl, *Angew. Chem., Int. Ed.*, 2009, **48**, 6543.
4 W. S. Hummers and R. E. Offeman, *J. Am. Chem. Soc.*, 1958, **80**, 1339.
5 X. Li, H. Wang, J. T. Robinson, H. Sanchez, G. Diankov and H. Dai, *J. Am. Chem. Soc.*, 2009, **131**, 15939.
6 J. I. Paredes, S. Villar-Rodil, A. Martínez-Alonso and J. M. D. Tascón, *Langmuir*, 2008, **24**, 10560.
7 L. G. Cançado, K. Takai, T. Enoki, M. Endo, Y. A. Kim, H. Mizusaki, A. Jorio, L. N. Coelho, R. Magalhães-Paniago and M. A. Pimenta, *Appl. Phys. Lett.*, 2006, **88**, 163106.
8 H. Yang, C. Shan, F. Li, D. Han, Q. Zhang and L. Niu, *Chem. Commun.*, 2009, 3880.
9 (*a*) S. R. Kelemen, M. Afeworki, M. L. Gorbaty and P. J. Kwiatek, *Energy Fuels*, 2002, **16**, 1507; (*b*) R. Pietrzak, *Fuel*, 2009, **88**, 1871; (*c*) G. Soto, E. C. Samano, R. Machorro, M. H. Farías and L. Cota-Araiza, *Appl. Surf. Sci.*, 2001, **183**, 246; (*d*) R. J. J. Jansen and H. van Bekkum, *Carbon*, 1995, **33**, 1021.
10 (*a*) S. Stankovich, D. A. Dikin, G. H. B. Dommett, K. M. Kohlhaas, E. J. Zimney, E. A. Stach, R. D. Piner, S. T. Nguyen and R. S. Ruoff, *Nature*, 2006, **442**, 282; (*b*) G. I. Titelman, V. Gelman, S. Bron, R. L. Khalfin, Y. Cohen and H. Bianco-Peled, *Carbon*, 2005, **43**, 641.
11 J. Shen, Y. Hu, M. Shi, X. Lu, C. Qin, C. Li and M. Ye, *Chem. Mater.*, 2009, **21**, 3514.
12 H. Kabashima, H. Tsuji, S. Nakatab, Y. Tanaka and H. Hattori, *Appl. Catal., A*, 2000, **194–195**, 227.

